Investigation of stacking faults in MOVPE-grown zincblende GaN by XRD and TEM

Lok Yi Lee[1, a], Martin Frentrup[1], Petr Vacek[1,2], Menno J Kappers[1], David J Wallis[1,3], and Rachel A Oliver[1]

[1] Department of Materials Science and Metallurgy, University of Cambridge, 27 Charles Babbage Road, Cambridge, CB3 0FS, United Kingdom

[2] Institute of Physics of Materials & CEITEC IPM, Academy of Sciences of the Czech Republic, Žižkova 22, 61600 Brno, Czech Republic

[3] Centre for High Frequency Engineering, University of Cardiff, 5 The Parade, Newport Road, Cardiff, CF24 3AA, United Kingdom

[a] Corresponding author: lyl24@cam.ac.uk

Abstract

X-ray diffraction and bright-field transmission electron microscopy are used to investigate the distribution and density of {111}-type stacking faults (SFs) present in a heteroepitaxial zincblende GaN epilayer with high phase purity, grown on a 3C-SiC/Si (001) substrate by metalorganic vapour-phase epitaxy. It is found that the 4° miscut towards the [110] direction of the substrate, that prevents the formation of undesirable antiphase domains, has a profound effect on the relative densities of SFs occurring on the different {111} planes. The two orientations of SFs in the [-110] zone, where the SF inclination angle with the GaN/SiC interface is altered by the 4° miscut, show a significant difference in density, with the steeper (111) SFs being more numerous than the shallower (-1-11) SFs by a factor of ~ 5 at 380 nm from the GaN/SiC interface. In contrast, the two orientations of SFs in the [110] zone, which is unaffected by the miscut, have densities comparable with the (-1-11) SFs in the [-110] zone. A simple model, simulating the propagation and annihilation of SFs in zincblende GaN epilayers, reproduces the presence of local SF bunches observed in TEM data. The model

also verifies that a difference in the starting density at the GaN/SiC interface of the two orientations of intersecting {111} SFs in the same zone reduces the efficiency of SF annihilation. Hence, (111) SFs have a higher density compared with SFs on the other three {111} planes, due to their preferential formation at the GaN/SiC interface caused by the miscut.

Keywords: GaN, cubic, zincblende, MOVPE, stacking fault, XRD, bright-field TEM

1. Introduction

In recent years, zincblende (zb) III-nitrides have attracted attention as a promising approach to improve the efficiencies of green-wavelength LEDs. In comparison to the hexagonal wurtzite (wz) phase, zb InGaN/GaN and AlGaN/GaN quantum well structures are in theory free of undesirable internal polarisation fields and the associated quantum confined Stark effect when grown in the (001) orientation, allowing for a higher recombination efficiency of electrons and holes. Furthermore zb-InGaN has a smaller bandgap than wz-InGaN of the same composition, alleviating the difficulties associated with the incorporation of In into InGaN quantum wells to achieve green-wavelength emission.

However, metastable zb-GaN suffers from a high density of {111} stacking faults (SFs) when grown on GaAs[1,2], 3C-SiC[3,4] and patterned 3C-SiC/Si[5] substrates. Such SFs are the dominant planar defect in zb-GaN and may negatively impact the optical and electronic properties of the material[6,7]. The SFs often originate from heteroepitaxial interfaces, where defects are generated to compensate for the lattice mismatch between the different materials.[8] SFs generated on the four different {111} planes in zb-GaN can interact with and annihilate each other, resulting in lower defect densities with increasing epilayer thickness.[4,6] The factors that

would affect the annihilation of SFs include the distribution and density of SFs on the different {111} planes.

Furthermore, zb-GaN grown on on-axis 3C-SiC/Si (001) substrates can suffer from the presence of antiphase domains, which are formed when zincblende SiC is grown on Si with the diamond crystal structure and are propagated into the subsequent GaN layer. The formation of such domains can be avoided by applying a 4° miscut to the Si substrate[9]. The impact of a 4° substrate miscut on the distribution and density of {111}-type SFs in zb-GaN epilayers, and the implication on the efficiency of SF annihilation to reduce SF density with increasing epilayer thickness have yet to be explored.

Here, we report on the influence of the substrate miscut on the distribution and density of {111}-type SFs present in a zb-GaN epilayer grown on a 3C-SiC/Si (001) substrate with a 4° miscut, using analyses by X-ray diffraction (XRD) and cross-sectional bright-field transmission electron microscopy (TEM). Based on the TEM experimental observations, a simple model of the SF propagation and annihilation in a zincblende epilayer was used to investigate the local distribution of SFs, and to determine how a difference in the densities of two orientations of intersecting {111} SFs at the GaN/SiC interface influences the SF density reduction with increasing epilayer thickness.

2. Experimental

The zb-GaN epilayer sample investigated was grown by MOVPE in a 6 × 2'' Thomas Swan close-coupled showerhead reactor on a ~ 2 × 2 cm^2 piece of a 150 mm diameter 3C-SiC/Si substrate provided by Anvil Semiconductors Ltd. The substrate consisted of a 2.9 μm thick layer of 3C-SiC grown on a 1000 μm thick Si (001) wafer with a nominal 4° miscut towards

the [110] in-plane direction. A thin GaN nucleation layer was followed by a ~ 380 nm thick zb-GaN epilayer grown under conditions which suppress the formation of the thermodynamically more stable wurtzite phase. The zb-GaN epilayer growth was carried out at a temperature of 875 °C, a V/III-ratio of 300 with a growth rate of approximately 1.8 μm h^{-1}. Trimethylgallium (TMG) and ammonia (NH_3) were used as Ga and N sources, and hydrogen was used as the carrier gas during growth[9].

XRD was used to investigate the zincblende phase purity and the global distribution of SFs in the GaN epilayer. A PANalytical Empyrean diffractometer equipped with a two-bounce hybrid monochromator (λ = 1.54056 Å), 1/4° primary beam slit, and a PIXcel solid-state area detector was used to obtain reciprocal space maps of the SF-related diffuse scattering around the on-axis 002 and off-axis 113-type zb-GaN and 3C-SiC reflections. The XRD measurements were performed in coplanar geometry, in the direction perpendicular to the miscut to investigate the SFs in the [110] zone, and parallel to the miscut to study the [-110] zone. Each measurement collected data from an area of ~ 2 cm^2, which is illuminated by the X-ray beam.

In order to investigate the local SF distribution, two cross-sectional TEM specimens were prepared where the zone axes were either (A) parallel or (B) perpendicular to the miscut direction by mechanical polishing and dimple grinding, followed by precision ion polishing with Ar^+ ions. Cross-sectional bright-field TEM was performed on a FEI Tecnai F20 operated at 200 kV to investigate a total of nine different regions from the two TEM specimens. The schematic in Figure 1 shows the (001)-oriented zb-GaN epilayer grown on a 3C-SiC/Si substrate with a miscut in the [110] direction. The black lines in the cross-sections of the GaN layer illustrate the alignment of the four different {111} SFs. The oppositely

inclined (-111) and (1-11) SFs which are edge-on when viewed in the [110] zone (shaded blue) are not directly affected by the substrate miscut and thus are both at a theoretical angle of 55° to the GaN/SiC interface. In contrast, the pair of oppositely inclined (-1-11) and (111) SFs which are edge-on when viewed in the [-110] zone (shaded green) have their relative angles to the GaN/SiC interface inclined by the 4° miscut: the (-1-11) SFs are at a shallower angle (51°) and the (111) SFs at a steeper angle (59°) with respect to the GaN/SiC interface. The density of a particular orientation of SF was determined at a distance of 380 nm from the GaN/SiC interface, with the consideration of the inclination angle of the SF with respect to the GaN/SiC interface such that the SF density calculated is reflective of the normal distance between the SFs.

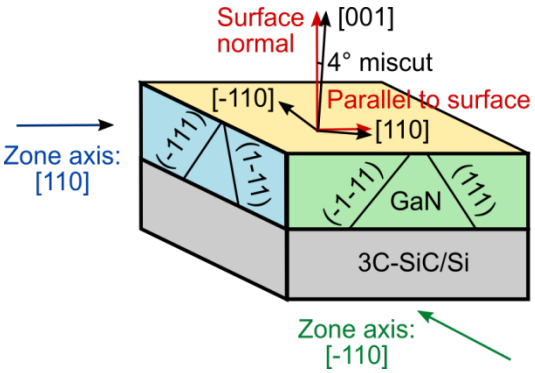

Figure 1 Schematic showing the alignment of the four {111}-type SFs in zb-GaN grown on a 3C-SiC/Si substrate with a 4° miscut towards [110]. The [110] zone is shaded blue, while the [-110] zone is shaded green.

3. Results and discussion

3.1. SF distribution in the [110] zone

First, we consider the SF distribution in the [110] zone, in which the inclination angle for both the (-111) and (1-11) SFs is 55° with respect to the GaN/SiC interface and is not affected by the substrate miscut.

Figure 2 shows the XRD reciprocal space maps of the off-axis (a) -113 and (b) 1-13 reflections, and (c) the on-axis 002 reflections of zb-GaN and 3C-SiC in the [110] zone, with the schematic in (d) illustrating their positions in reciprocal space. The low-intensity streaks along the <111> directions that pass through the reflections are caused by diffuse scattering on the {111}-type SFs. The degree of broadening of a reflection is believed to depend strongly on the density of SFs[10]. Since a SF always produces diffuse scattering in the directions normal to its plane, it is possible to attribute a streak to a particular orientation of SF and hence qualitatively compare the densities between the two {111}-type SFs in the zone. The yellow circles in Figure 2 mark the expected positions of wurtzite reflections, which are absent in all three reciprocal space maps, revealing that the zb-GaN epilayer has a high phase purity. It is interesting to note that the SF streaks are not perfectly symmetric about the zb reflections along <111>, but always have a larger broadening on the side of the expected nearest wz reflections on the <111> streaks. This is due to the mixed wz and zb stacking of randomly-spaced SFs leading to an enhanced diffuse scattering in between the zb reflections and expected wz reflections.

The 002 zb-GaN reflection in Figure 2 (c) is broadened to a 4-pointed star-like shape. It is fairly mirror-symmetrical about the Q_z-axis, and the (1-11) and (-111) SF streaks have similar intensities. This indicates a similar density of the (1-11) and (-111) SFs in the sample. The higher background intensity in the bottom left part of the reciprocal space map ($Q_x < 0.3$) in Figure 2 (c) is caused by diffuse scattering from surface features as the incident beam was at an angle of ~2° to the sample surface. However this does not affect the interpretation of the SF scattering, since there is sufficient distance between the surface scattering and the 002 zb-GaN reflection spot. The observations made from the 002 reflection are also seen from the -

1-13 and 113 zb-GaN reflections in Figure 2 (a) and (b) respectively. Both 113-type reflections are broadened in the directions of the SF streaks, and are mirror-symmetrical about the surface normal Q_z. Since XRD collects data from a large area of the sample, the results reveal that there is no global preference of the SF inclination in the [110] zone, indicating similar densities of (1-11) and (-111) SFs.

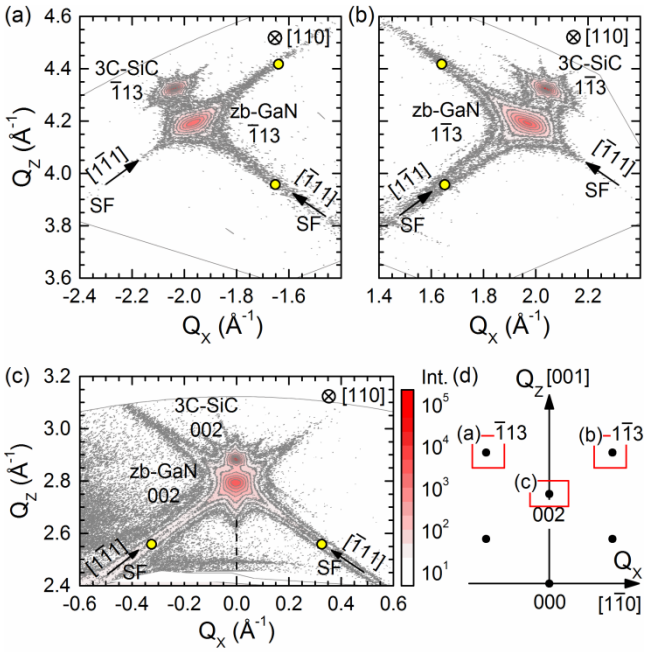

Figure 2 XRD reciprocal space maps showing the (a) -113, (b) 1-13, and (c) 002 reflections of zb-GaN and 3C-SiC in the [110] zone, where Q_x and Q_z are parallel and normal to the sample surface respectively. The yellow circles mark the expected positions of wz-GaN reflections, in the case of phase contamination. (d) A schematic illustrating the positions of the reflections in reciprocal space.

To gain an insight into the local defect distribution, TEM was used to investigate the distribution and density of the different orientations of SFs in the [110] zone. Figure 3 shows the cross-sectional bright-field TEM images (zone axis = [110], g = -111) of two of the regions studied. The planar SFs are visible as dark lines running through the thickness of the

epilayer. The yellow solid lines highlight examples of (-111) and (1-11) SFs, which are both inclined at 55° from the GaN/SiC interface (white dotted line). The density of SFs near the GaN/SiC interface is very high, but as a result of annihilation, there is a large reduction in SF density within the first 100 nm of the GaN epilayer. Close to the surface of the ~ 380 nm thick epilayer, both orientations of SFs are not distributed evenly and often occur as bunches, as indicated by the arrows in Figure 3.

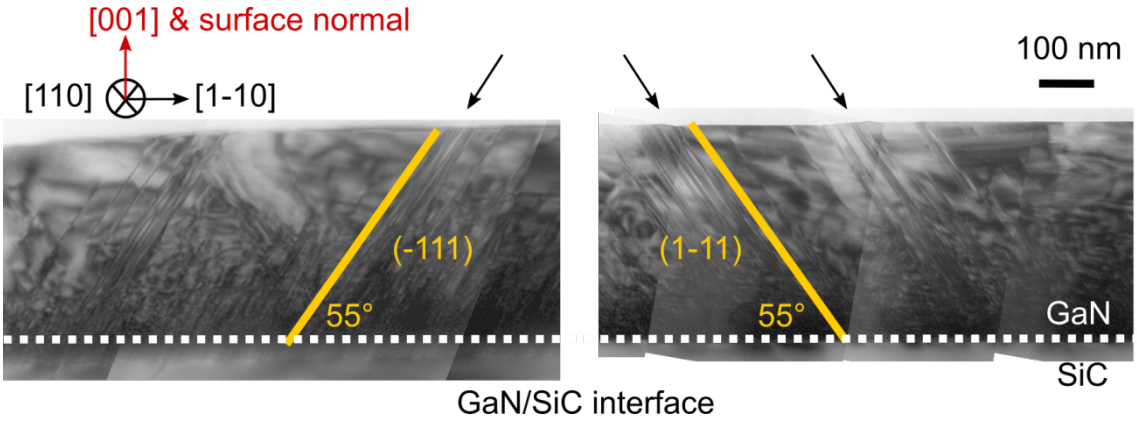

Figure 3 Cross-sectional bright-field TEM images of the GaN epilayer with zone axis = [110], g = -111, where the SFs appear as dark lines. The yellow lines highlight the inclinations of the (-111) and (1-11) SFs with respect to the GaN/SiC interface, and the arrows indicate bunches of SFs.

The properties of SFs close to the surface of the 380 nm thick epilayer from four distinct regions of the sample with a total length of 11.2 µm were studied quantitatively. For example, for the TEM images shown in Figure 3 with a total length of 2.06 µm, 45 SFs are clearly identifiable in the GaN epilayer measured at distance of 380 nm from the GaN/SiC interface. Note that SFs separated by less than 4 nm cannot be resolved from the TEM images, and hence were counted as a single SF. SF bunches in the four regions contained between 4 and 17 SFs, and the average distance between SFs within a bunch is 16 nm.

Table 1 provides a summary for each of the four regions studied in the [110] zone, including their length, the ratio of the number of (-111) SFs to the number of (1-11) SFs, and the total SF density. The local density of a particular orientation of SF varies strongly: in three regions (A1 to A3), there are more (-111) SFs than (1-11) SFs. However, in region A4, there are significantly more (1-11) SFs than (-111) SFs. The total SF density does not differ significantly between the four regions and varies from 2.4×10^5 cm $^{-1}$ to 3.0×10^5 cm $^{-1}$. The average SF density of the four regions weighted by their respective lengths is $(2.8 \pm 0.1) \times 10^5$ cm $^{-1}$, while the average density of (-111) SFs and (1-11) SFs are $(1.8 \pm 0.6) \times 10^5$ cm $^{-1}$ and $(0.9 \pm 0.6) \times 10^5$ cm $^{-1}$, respectively. The errors quoted here are the standard error of the mean of the measurements from the four regions.

The results of the TEM analysis show that there is a local anisotropy in the SF inclination. Although somewhat limited by the sampling area of TEM, our results also suggest that there is no global preference for (-111) or (1-11) SFs, supporting the results from the XRD analysis. Later, in Section 3.3, we will use a model to simulate the possibility of a local anisotropy in the SF inclination, arising from the formation of SF bunches in a material which has no global anisotropy of SF inclination.

Region	**Length parallel to GaN/SiC interface (μm)**	**No. of (-111) : No. of (1-11) SFs**	**Total SF density ($\times 10^5$ cm $^{-1}$)**
A1	4.9	6.1 : 1	3.0
A2	2.9	4.8 : 1	2.7
A3	1.7	16 : 1	2.4
A4	1.7	1 : 12	2.9

Table 1 Summary of the results obtained from the TEM analysis of the [110] zone from four distinct regions.

3.2. SF distribution in the [-110] zone

Next, we consider the SF distribution in the [-110] zone, in which the inclination angle of the (-1-11) and (111) SFs with respect to the GaN/SiC interface is affected by the 4° substrate miscut.

Figure 4 shows the XRD reciprocal space maps of the off-axis (a) -1-13 and (b) 113 reflections, and (c) the on-axis 002 reflections of zb-GaN and 3C-SiC in the [-110] zone, with the schematic in (d) illustrating their positions in reciprocal space. Due to the miscut, the reflections are tilted by 4° about the [-110] zone axis. This is apparent from a comparison of the schematics in Figure 2 (d) and Figure 4 (d) which show the positions of the 002 and 113-type reflections. The axes Q_y and Q_z represent the directions parallel and normal to the sample surface respectively, and thus do not coincide perfectly with the [110] and [001] crystal axes due to the 4° substrate miscut. The 4° tilt of the 002 reflection away from the surface normal is marked in the reciprocal space map in Figure 4 (c).

In contrast to the [110] zone, the 4-pointed star-like shape of the 002 reflection in Figure 4 (c) is not mirror-symmetrical along the Q_z-axis but broadened along the [111] direction, and the (-1-11) SF streak has a significantly lower intensity than the (111) SF streak. A similar anisotropy in the broadening of reflections can be observed in the reciprocal space maps of the -1-13 and 113 zb-GaN reflections in Figure 4 (a) and (b) respectively, where the (111) SF streak is more intense than the (-1-11) SF streak.

Hence from XRD analysis, we can conclude that there is a global anisotropy in SF inclination in the [-110] zone, with a significantly higher density of (111) SFs compared with (-1-11) SFs. From the rotation of the reflections and SF streaks in the reciprocal space map, we can determine that SFs tend to form preferentially on the steeper {111} plane with respect to the growth surface.

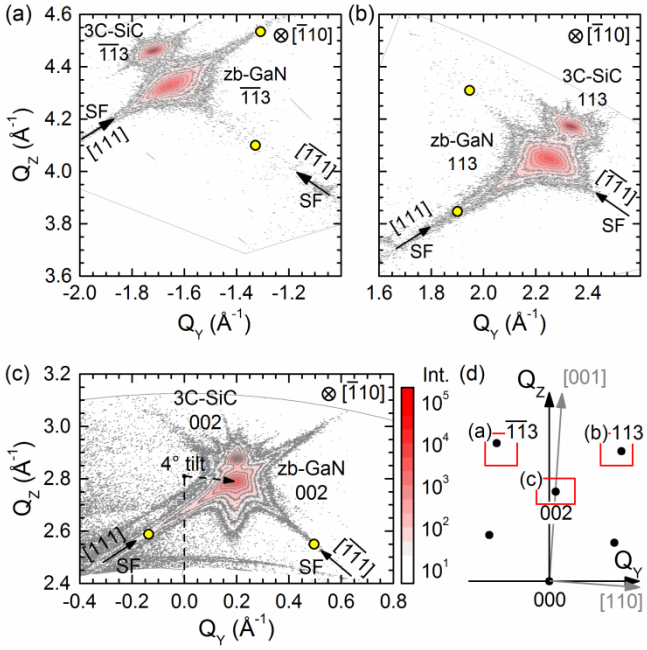

Figure 4 XRD reciprocal space maps showing the (a) -1-13, (b) 113, and (c) 002 reflections of zb-GaN and 3C-SiC in the [-110] zone. The yellow circles mark the expected positions of wz-GaN reflections, in the case of phase contamination. (d) A schematic illustrating the positions of the reflections in reciprocal space.

The observations made by XRD are also supported by the TEM analysis. A cross-sectional bright-field TEM image of a region of the GaN epilayer with zone axis = [-110], g = 111 is shown in Figure 5. The yellow solid lines highlight examples of (-1-11) and (111) SFs, which are at ~ 51° and ~ 59° respectively to the GaN/SiC interface (black dotted line); the different inclination angles of the SFs in the [-110] zone are a result of the substrate miscut, as

observed in XRD measurements. Note that parts of the GaN/SiC interface and the first 100 nm of the GaN epilayer were milled away during the TEM sample preparation. However, the same two main observations made from the TEM image of the [110] zone (Figure 3) can be made in the TEM images of the [-110] zone (Figure 5): the high density of SFs in GaN close to the GaN/SiC interface rapidly decreases within the first 100 nm of the epilayer, and the occurrence of SF bunches close to the surface of the epilayer.

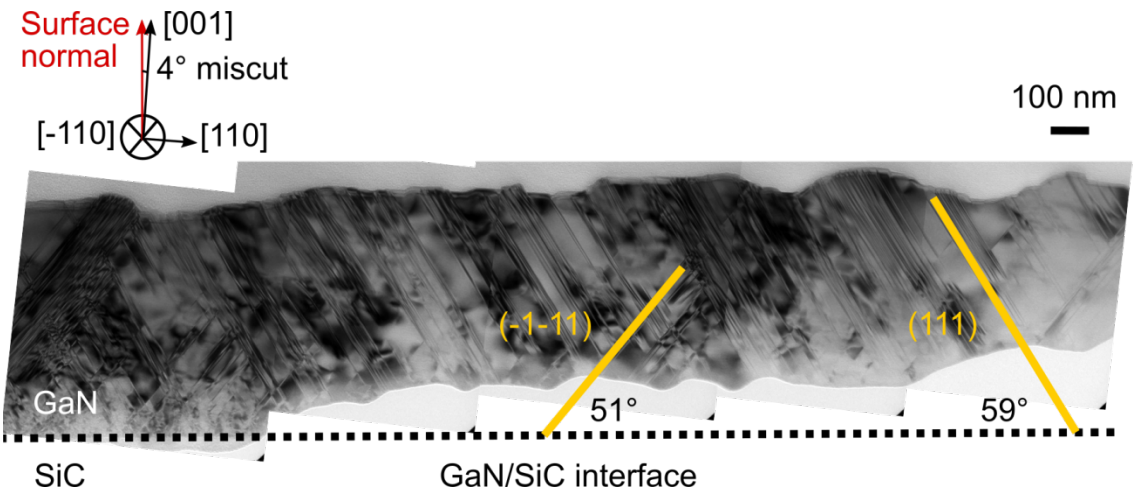

Figure 5 Cross-sectional bright-field TEM image of the GaN epilayer with zone axis = [-110], g = 111. The yellow lines highlight the inclinations of the (-1-11) and (111) SFs with respect to the GaN/SiC interface.

The number and orientation of SFs close to the surface of the 380 nm thick epilayer from five distinct regions of the sample with a total length of 10.2 µm were studied. For example, for the TEM image shown in Figure 5 with a total length of 2.9 µm, 155 (111) SFs and only 20 (-1-11) SFs are clearly identifiable in the GaN layer at a thickness of ~ 380 nm. Table 2 provides a summary of the approximate length of each region studied, the ratio of the number of (-1-11) SFs to the number of (111) SFs, and the total SF density. In all five regions of the sample studied, there are significantly more (111) SFs than (-1-11) SFs, with ratio of (-1-11)

to (111) ranging from 1 : 3 to 1 : 29, suggesting a global anisotropy in the SF inclination. There is a significant range in the total SF density between the five regions, from 4.8×10^5 cm $^{-1}$ to 9.4×10^5 cm $^{-1}$, due to the presence of SF bunches in regions B4 and B5. The average SF density across all five regions, weighted by the length of each region, is $(6.5 \pm 1.0) \times 10^5$ cm $^{-1}$, while the average density of (-1-11) SFs and (111) SFs are $(1.1 \pm 0.2) \times 10^5$ cm $^{-1}$ and $(5.8 \pm 1.0) \times 10^5$ cm $^{-1}$, respectively. The error quoted for the SF density values is the standard error of the mean of the measurements from the five regions.

Region	**Length parallel to GaN/SiC interface (μm)**	**No. of (-1-11) : No. of (111) SFs**	**Total SF density ($\times 10^5$ cm $^{-1}$)**
B1	4.7	1 : 3.4	5.2
B2	1.3	1 : 3.0	6.3
B3	1.1	1 : 4.1	4.8
B4	1.6	1 : 6.4	9.4
B5	1.6	1 : 29	9.0

Table 2 Summary of the results obtained from the TEM analysis of the [-110] zone from five distinct regions.

Comparing all four orientations of {111} SFs across both zones in Table 3, the average density of (111) SFs of $(5.8 \pm 1.0) \times 10^5$ cm $^{-1}$ is significantly higher than that of the other three orientations of SFs, which range from 0.9×10^5 cm $^{-1}$ to 1.8×10^5 cm $^{-1}$. Due to the miscut, the (111) plane is the steepest {111} plane with respect to the GaN/SiC interface. Hence the results from both XRD and TEM lead to the same observation: SF formation occurs more frequently on the {111} plane with the steepest angle to the GaN/SiC interface, and the mis-orientation of the growth surface has a significant influence on the SF density. One possible explanation for the influence of the miscut on the SF density might be that on

the miscut SiC surface, step bunches form with {111} microfacets and SFs are preferentially formed on these facets. However, this would be expected to lead to increased stacking fault density on the shallower {111} facet, and not on the steeper facet as we observe in experiments. An alternative explanation might involve differences in strain relaxation mechanisms parallel and perpendicular to the miscut direction, and we are still investigating this possibility.

Zone axis	SF plane	Density ($\times 10^5$ cm^{-1})
[110]	(-111)	1.8 ± 0.6
[110]	(1-11)	0.9 ± 0.6
[-110]	(-1-11)	1.1 ± 0.2
[-110]	(111)	5.8 ± 1.0

Table 3 Summary of the average density of all four orientations of {111} SFs in the zb-GaN epilayer at a distance of 380 nm from the GaN/SiC interface, obtained from cross-sectional bright-field TEM images with zone axes [110] and [-110].

The significantly higher density of (111) SFs compared to the other three ((-1-11), (-111), (1-11)) may originate from a preferential formation of (111) SFs during the initial stages of GaN growth, making it less likely for these planar defects to intersect with opposing (-1-11) SFs and annihilate. In Section 3.3, we use an SF annihilation and propagation model to test whether this hypothesis is consistent with our observations.

3.3. Modeling of the SF annihilation

Our cross-sectional bright-field TEM analysis of the sample shows that when SFs on oppositely inclined {111} planes meet, e.g. when a (-1-11) SF intersects with a (111) SF, there are three possibilities: (a) the two SF lines annihilate each other, (b) one of the SF lines

is annihilated while the other propagates through the intersection point, or (c) both of the SF lines propagate, as indicated by the yellow arrows in Figure 6. It is possible that each line consists of more than one SF, since the minimum separation between SFs that can be resolved from the TEM images shown here is 4 nm, and SF separations less than this have been observed in zb-GaN epilayers by high-resolution TEM data previously[11]. Hence for Figure 6 (b), it could be the case that two SFs intersect with one oppositely inclined SF, resulting in the annihilation of only a pair of SFs. We developed a SF propagation and annihilation model to investigate how the preferential formation of one orientation of {111} SF affects the reduction in SF density with increasing epilayer thickness. The model uses a two-dimensional projection of a face-centred cubic (fcc) lattice viewed from <110> direction and only considers SFs of the same zone. The interactions between both intrinsic and extrinsic SFs are modelled by reactions of Shockley partial dislocations that commonly bound SFs in fcc materials[12], and we have observed Shockley partials dislocations experimentally in our zb-GaN samples by high-resolution scanning TEM. Each SF generated at the SiC/GaN interface is randomly assigned to one of the two {111} planes, and to one of six possible Shockley partial dislocations with Burgers vectors $\mathbf{b}$ = 1/6 <112> on the {111} plane. The spacings between SFs at the SiC/GaN interface are assumed to have a normal distribution described by the mean distance and variance, which are used as input parameters of the model. With increasing epilayer thickness, the SFs are modelled to propagate on {111} planes. At the intersection of two SFs, Frank's rule is applied to determine whether it is energetically favourable for the two partial dislocations associated with the SFs with Burgers vectors $\mathbf{b}_1$ and $\mathbf{b}_2$ to react and form a new dislocation with Burgers vector $\mathbf{b}_3$.[12] If the reaction is energetically favourable ($|\mathbf{b}_3|^2 < |\mathbf{b}_1|^2 + |\mathbf{b}_2|^2$), the two SFs annihilate each other; if the reaction is energetically unfavourable ($|\mathbf{b}_3|^2 \geq |\mathbf{b}_1|^2 + |\mathbf{b}_2|^2$), the two SFs continue to propagate into the epilayer. Since the model is two-dimensional and only considers reactions between

SFs on oppositely inclined {111} planes of the same zone, it does not cover all the possible reactions between dislocations on all four {111} planes. It might also be beneficial to take into account the SF energies in zb-GaN; however, such energies have been estimated to be small and negative[13] and in order to keep our model simple, we have not considered them here. Despite these simplifications, the model is sufficient to make predictions on the distribution and density of SFs. To be statistically relevant, a significant number of SFs should be present at the surface of the simulated film. This is influenced by the width and thickness of the film and the initial configuration of the SFs at the interface. Typically our simulated films have at least several 10s of SFs at the surface.

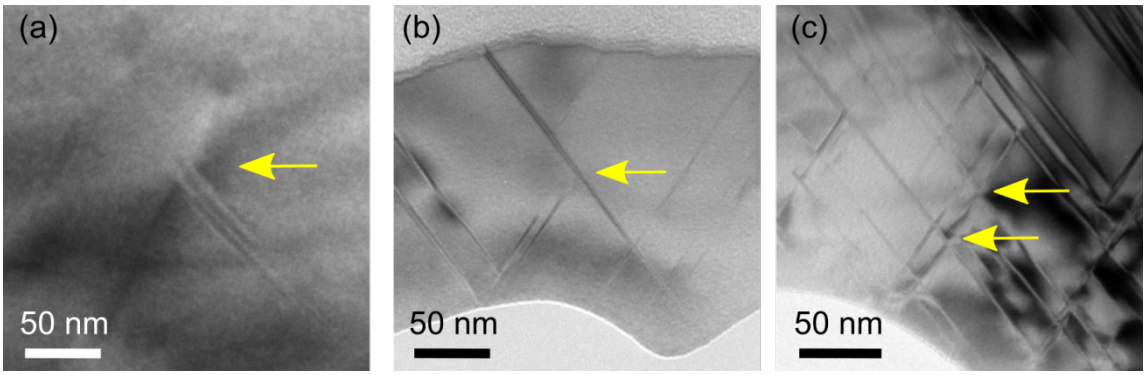

Figure 6 Cross-sectional bright-field TEM images of the zb-GaN epilayer with the yellow arrows indicating the three possibilities when oppositely inclined {111} SF lines intersect: (a) the two SF lines annihilate each other, (b) one of the SF lines is annihilated while the other propagates through, and (c) both SF lines propagate through.

Using our SF propagation and annihilation model, we simulated a 400 nm thick and ~ 3.5 µm wide GaN epilayer, with a total of 720 SFs that have a mean separation of 4.78 nm parallel to the GaN/SiC interface (equal to a total SF density of about 2.6×10^6 cm^{-1}) and the variance of the separations is 0.40 nm.

We first simulated the case where the ratio between the two oppositely inclined {111} SFs at the GaN/SiC interface, or the '*starting SF anisotropy*', is 1. The simulation was repeated multiple times to generate different defect arrangements in the GaN epilayer, and a typical result of the simulation is presented in Figure 7 (a). In this example, the SF density at the GaN/SiC interface is 2.6×10^6 cm^{-1} and reduces dramatically within the first 100 nm of the GaN epilayer by a factor of 5 to 0.5×10^6 cm^{-1}, reflecting the TEM experimental observations. More significantly, one can observe bunches of both orientations of oppositely inclined {111} SFs close to the surface of the 400 nm thick epilayer, even when the densities of the two orientations of SFs at the GaN/SiC interface are similar. This highlights that even if the SF inclination is essentially isotropic globally in the epilayer, a local anisotropy of inclination due to the presence of SF bunches can result from a normal distribution of the separation between SFs at the GaN/SiC interface. The results of this model are consistent with our observations of the SFs in the [110] zone from both XRD and TEM.

The situation changes when the densities of the two orientations of oppositely inclined SFs are dissimilar at the GaN/SiC interface, as illustrated in Figure 7 (b) where the starting SF anisotropy is 1.5. As with the previous case, a large number of SFs are annihilated within the first 100 nm of the GaN epilayer as they intersect with oppositely inclined SFs. However, with increasing epilayer thickness, bunches of the same orientation of SF preferentially formed at the GaN/SiC interface dominate, since there are not enough of the oppositely inclined SFs in the vicinity to allow annihilation to proceed. The more dominant SF bunches continue to propagate through the thickness of the epilayer and no further reduction in SF density occurs globally. The results of the model in this case are also consistent with our observations of the SFs in the [-110] zone from both XRD and TEM.

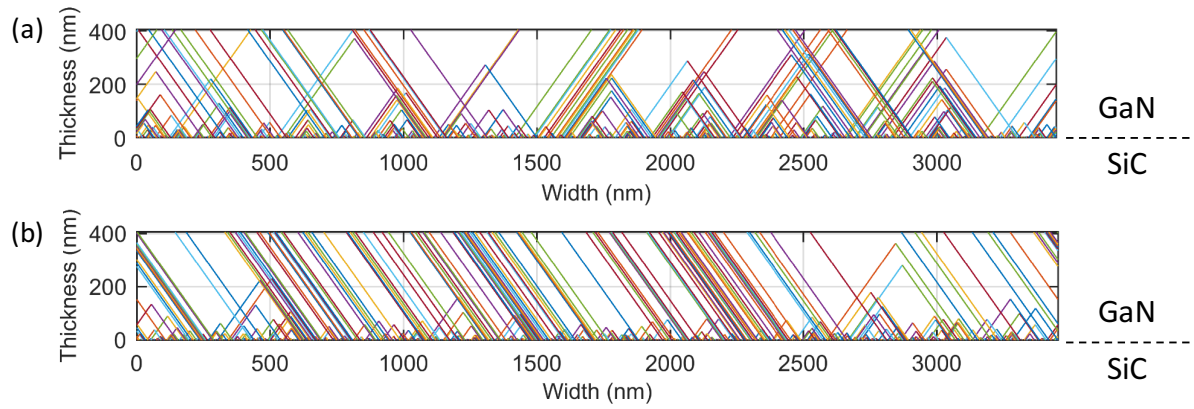

Figure 7 Simulation of SF annihilation in a zincblende epilayer that is 400 nm thick and ~ 3.5 µm wide, with (a) no starting SF anisotropy and (b) a 3:2 starting SF anisotropy.

To investigate the effect of a disparity in the density of oppositely inclined SFs at the GaN/SiC interface on the reduction in SF density with epilayer thickness, we simulated the SF densities at a thickness of 380 nm for different starting SF anisotropies. The SF density at the GaN/SiC interface was kept constant at 2.6×10^6 cm^{-1}, by defining the input parameters of the model SF separation mean and variance to be 4.78 nm and 0.40 nm respectively. Each data point in Figure 8 is the average of 10 different SF configurations for a given starting SF anisotropy, and the error bars shown represent the standard error of the mean. The simulations show that the isotropic case, where the starting SF anisotropy is 1, results in the lowest SF density at the surface of the GaN epilayer. However, as the degree of the starting anisotropy increases and the starting SF anisotropy differs from 1, the SF density measured at a thickness of 380 nm increases. Such results are consistent with the TEM data, where the [110] zone with notionally no starting SF anisotropy has a lower SF density at 380 nm away from the interface than the [-110] zone with an anisotropy related to the miscut. The results also support our hypothesis that a disparity in the density of oppositely inclined SFs at the GaN/SiC interface results in a lower chance of annihilation for the orientation of SF that has

a higher starting density, thus reducing the efficiency of the SF annihilation process, and limiting the reduction in SF density with epilayer thickness.

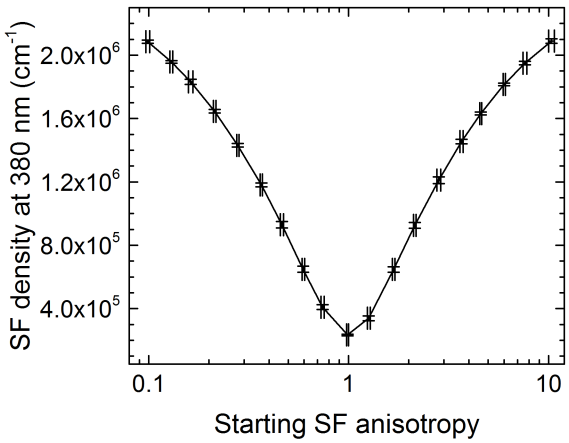

Figure 8 Plot of simulated SF densities for a GaN epilayer at a thickness of 380 nm against the starting SF anisotropy. The SF density at the GaN/SiC interface is 2.6×10^6 cm^{-1}. Note the logarithmic scale of the x-axis.

4. Conclusions

The formation of APDs in zincblende GaN grown on 3C-SiC/Si substrates was successfully suppressed by using substrates with a 4º miscut toward [110]. XRD and TEM results both show a higher SF density in the [-110] zone than the [110] zone of the zincblende GaN epilayer, and that this global anisotropy in SF inclination is caused by a higher density of SFs lying on the steeper {111} plane to the GaN/SiC interface. A model simulating the SF propagation and annihilation confirms the occurrence of local SF density fluctuations due to the formation of bunches of one orientation of SF while the SF density remains isotropic globally, as was experimentally observed. The model further shows that a difference in the density of oppositely inclined SFs at the GaN/SiC interface results in a significantly higher density near the GaN surface at a thickness of 380 nm of the orientation of SF that had a higher starting density at the interface. The combined experimental and theoretical results

imply that the miscut of the substrate affects the relative densities of {111}-type SFs generated at the GaN/SiC interface, reduces the efficiency of the SF annihilation process, and hence the global reduction of SF density with increasing epilayer thickness. For a good balance between preventing the formation of APDs and efficient SF annihilation, further investigation on a miscut series is required to find an optimal miscut angle. If, in the development of SiC/Si substrates, it proves impossible to avoid APD formation without introducing a miscut, then our results suggest that the miscut will define the minimum stacking fault density which can be achieved by increasing the layer thickness. Therefore, other methods of stacking fault density reduction will need to be explored, either in terms of changes to the nucleation layer which reduces the starting stacking fault density, or alternative methods to block stacking fault propagation through the layer.

Acknowledgements

We would like to thank Innovate UK for the financial support within the Energy Catalyst Round 4 - Mid Stage Feasibility scheme (Ref. 102766), and EPSRC for support through grant no. EP/M010589/1 and grant no. EP/R01146X/1. P Vacek would like to thank the Ministry of Education, Youth and Sports of the Czech Republic for supporting a 6-month research stay at the Cambridge Centre for Gallium Nitride through the project no. CZ.02.2.69/0.0/0.0/16_027/0008056. DJ Wallis would like to acknowledge support from EPSRC Manufacturing fellowship, EP/N01202X/2.

References

[1] A. Trampert, O. Brandt, and K.H. Ploog, Angew. Chem. Int. Ed. Engl. **36**, 2111 (1997).

[2] D. Chandrasekhar, D.J. Smith, S. Strite, M.E. Lin, and H. Morkoç, J. Cryst. Growth **152**, 135 (1995).

[3] D.J. As, R. Kemper, C. Mietze, T. Wecker, J.K.N. Lindner, P. Veit, D. A, F. Bertram, and J. Christen, Mater. Res. Soc. Symp. Proc. **1736**, (2014).

[4] E. Martinez-Guerrero, E. Bellet-Amalric, L. Martinet, G. Feuillet, B. Daudin, H. Mariette, P. Holliger, C. Dubois, C. Bru-Chevallier, P.A. Nze, T. Chassagne, G. Ferro, and Y. Monteil, J. Appl. Phys. **91**, 4983 (2002).

[5] R.M. Kemper, M. Weinl, C. Mietze, M. H, T. Schupp, E. Tschumak, J.K.N. Lindner, K. Lischka, and D.J. As, J. Cryst. Growth **323**, 84 (2011).

[6] R.M. Kemper, P. Veit, C. Mietze, A. Dempewolf, T. Wecker, F. Bertram, J. Christen, J.K.N. Lindner, and D.J. As, Phys. Status Solidi C **12**, 469 (2015).

[7] S.A. Church, S. Hammersley, P.W. Mitchell, M.J. Kappers, S.L. Sahonta, M. Frentrup, D. Nilsson, P.J. Ward, L.J. Shaw, D.J. Wallis, C.J. Humphreys, R.A. Oliver, D.J. Binks, and P. Dawson, Phys. Status Solidi **254**, 1600733 (2017).

[8] A. Trampert, O. Brandt, H. Yang, and K.H. Ploog, Appl. Phys. Lett. **70**, 583 (1997).

[9] L.Y. Lee, M. Frentrup, M.J. Kappers, R.A. Oliver, C.J. Humphreys, and D.J. Wallis, J. Appl. Phys. **124**, 105302 (2018).

[10] M. Barchuk, V. Holý, D. Kriegner, J. Stangl, S. Schwaiger, and F. Scholz, Phys. Rev. B **84**, 1 (2011).

[11] S.A. Church, S. Hammersley, P.W. Mitchell, M.J. Kappers, L.Y. Lee, F. Massabuau, S.L. Sahonta, M. Frentrup, L.J. Shaw, D.J. Wallis, C.J. Humphreys, R.A. Oliver, D.J. Binks, and P. Dawson, J. Appl. Phys. **123**, 185705 (2018).

[12] D. Hull and D.J. Bacon, in *Introd. to Dislocations*, Fifth Edit (Butterworth-Heinemann, 2011), pp. 85–107.

[13] A.F. Wright, J. Appl. Phys. **82**, 5259 (1997).